Energetics and structures of neutral and charged Si_n ($n \leq 10$) and sodium-doped Si_nNa clusters

Siqing Wei, R. N. Barnett, and Uzi Landman

School of Physics, Georgia Institute of Technology, Atlanta, Georgia 30332-0430

(Received 18 September 1996)

Energetics and structures of neutral and charged Si_n ($n \leq 10$) and sodium-doped Si_nNa clusters have been investigated using local spin density functional electronic structure calculations and structural optimizations, with and without exchange-correlation gradient corrections. For the Si_n clusters, the monomer separation energies show local maxima for $n=4$, 7, and 10. The vertical and adiabatic ionization potentials are smaller than the values for the Si atom and exhibit odd-even oscillations with values in agreement with experiments, and the adiabatic electron affinities show local minima for $n=4$, 7, and 10, with the value for the heptamer being the smallest, in agreement with the experimentally measured pattern. Binding of Na to Si_n is characterized by charge transfer from the sodium resulting in the development of significant dipole moments for the Si_nNa clusters. The binding energy of Na to Si_n oscillates as a function of n, with local maxima for $n=2$, 5, and 9, and local minima for $n=4$, 7, and 10, with the value for $n=7$ being the smallest. A similar trend is found for the vertical and adiabatic ionization potentials of the doped clusters, correlating with the electron affinity trend exhibited by the Si_n clusters, and in agreement with recent measurements. In the optimal adsorption geometry of H_2O on the Si_7Na cluster, the oxygen is bonded to the Na, with a hydration energy significantly higher than that of an isolated sodium atom. The vertical and adiabatic ionization potentials of NaH_2O are lower than those of Si_7NaH_2O, and the values for the latter are lower, by ≈ 0.2 eV, than those of the unhydrated Si_7Na cluster. [S0163-1829(97)05211-9]

I. INTRODUCTION

Investigations of the geometries, electronic structures, energetics, and reactivities of atomic clusters have attracted significant interest in recent years. One of the principal goals of these research activities is to explore the size evolutionary patterns of the properties of materials aggregates from the molecular to the condensed phase regimes.

Small covalently bonded elemental semiconductors clusters (such as C, Si, and Ge) have been the subject of increasing theoretical[1-19] and experimental[20-30] research efforts since their properties are rather different from those of the bulk material. In particular, small Si_n clusters have been investigated employing several theoretical approaches. These include quantum chemistry methods,[1,2,5,8,19] tight-binding models,[4,13,14,15] calculations based on the local-density-functional method,[6,9-11,16,17] and variational fixed-node diffusion Monte Carlo studies.[18] For some small Si_n clusters the ground-state geometries have been determined experimentally,[29] confirming the theoretically proposed ones[5] (for $n=2$–7).

Recently, the ionization potentials of sodium-doped silicon clusters (Si_nNa_m, $3 \leq n \leq 11$, $1 \leq m \leq 4$), have been measured,[31] and certain aspects of the geometrical and electronic structure of Si_nNa ($1 \leq n \leq 7$) clusters have been studied.[32] It has been found in the experiments [see Ref. 31, Fig. 1(a) and Fig. 2 in Ref. 32] that the ionization threshold energies for Si_nNa clusters with $n=4$, 7, and 10 are local minima, correlating with the measured[26] low values of the electron affinity of bare silicon clusters, Si_n^-, with $n=4$, 7, and 10. This suggests that the valence electron of the Na atom in the doped Si_nNa clusters may be treated as an "excess" electron, "donated" to the Si_n host.

In this study we have investigated the energetic and structural properties of bare Si_n, Si_n^+, Si_n^- ($n \leq 10$) clusters and of Na-doped Si_nNa and Si_nNa^+ ($n \leq 10$) clusters. In these calculations we have used structural optimizations and molecular dynamics (MD) simulations using the Born-Oppenheimer (BO) local-spin-density (LSD) functional MD method[33] (BO-LSD-MD), with and without exchange-correlation gradient corrections. Following a brief description of the calculation method in Sec. II, we present our results in Sec. III, and summarize our findings in Sec. IV, including a discussion of water adsorption on the Si_7Na cluster.

II. METHOD

In calculations of the total energies and structural optimizations we have used the BO-LSD-MD method,[33] where the motion of the ions is confined to the ground-state BO electronic potential energy surface calculated concurrently via the Kohn-Sham (KS)–LSD method. In these calculations we have employed nonlocal norm-conserving pseudopotentials[34] for the valence electrons of the silicon and sodium atoms (s, p, and d components, with s and p nonlocalities); in simulations involving water (see Sec. IV), s and p components were used for the oxygen atom, and a local pseudopotential for the hydrogens.[33]

As discussed in details elsewhere,[33] in our method no supercells (i.e., periodic replica of the ionic system) are used thus allowing studies of charged and multipolar clusters in an accurate and straightforward manner. In structural optimizations, using a conjugate gradient method, and in dynamical simulations, the Hellmann-Feynman forces on the ions are evaluated between each optimization, or MD step, involving
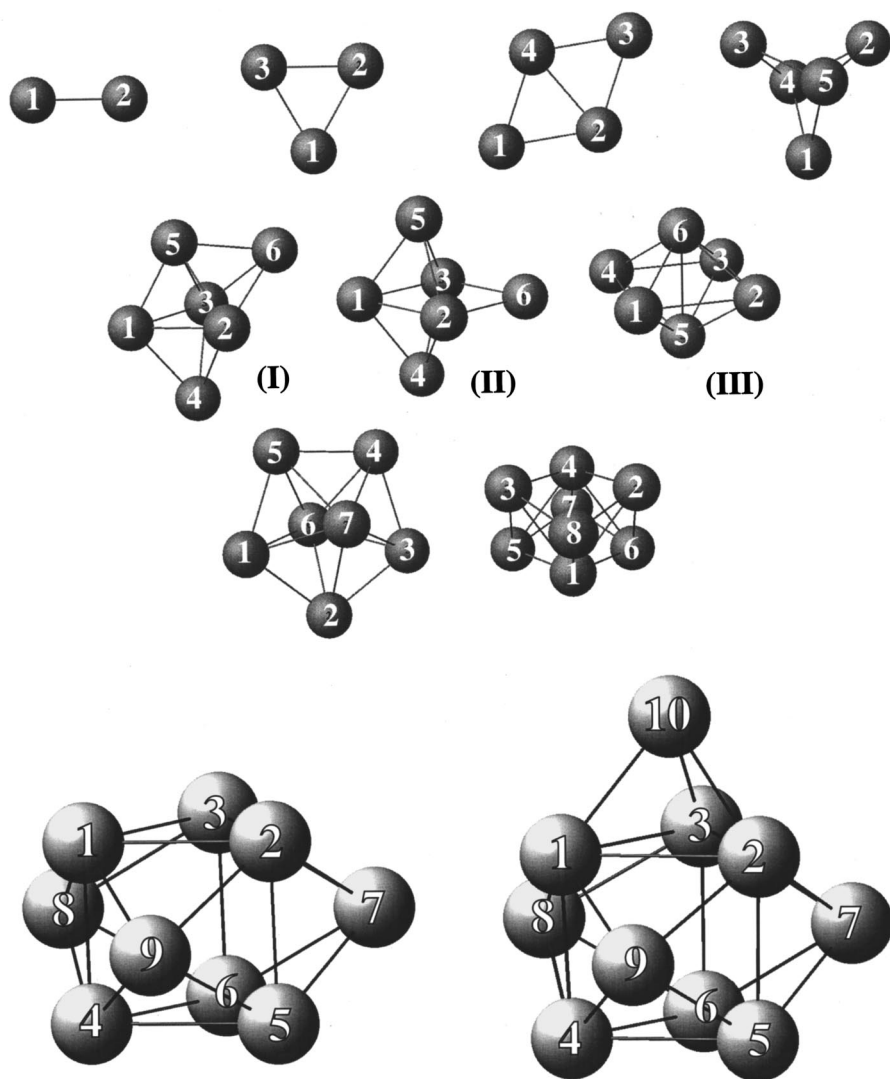
FIG. 1. Optimal geometries for neutral Si_2–Si_{10} clusters. For Si_6 three isomers are shown, I, II, and III in order of decreasing stability [the total energy of Si_6(II) and (III) are higher than that of Si_6(I) by 16 and 113 meV, respectively]. For values of interatomic distances see Table IV, where the numbering of the atoms is as shown in the figure.

iterative solution of the KS-LSD equations, thus insuring that the ionic trajectories are followed on the BO potential energy surface. Both LSD calculations and calculations including exchange-[35] correlation[36] gradient corrections (xcg) have
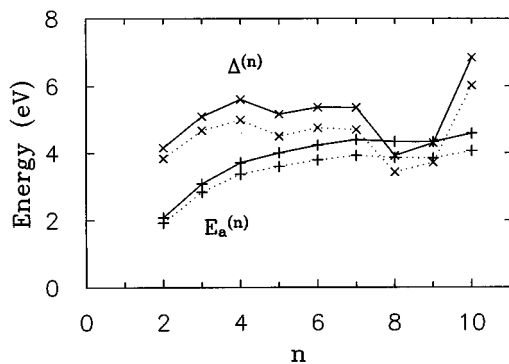
been performed (the xcg calculations were performed in the post LSD mode, PLSD, i.e., the gradient corrections were evaluated using the charge densities and optimized geometries obtained via the LSD calculations). A plane-wave cut-off of 20 Ry was used in calculations of Si_n and Si_nNa clusters, and a larger cutoff (62 Ry) was employed in the

FIG. 2. Atomization energy, $E_a^{(n)} = (E^{(n)} - nE^{(1)})/n$, where $E^{(n)}$ is the total energy of Si_n, and monomer separation energies, $\Delta^{(n)} = E^{(n+1)} - E^{(n)} - E^{(1)}$, for $1 \leq n \leq 9$, i.e., Si_2–Si_{10}. Energies in units of eV are given from LSD (solid) and PLSD (including exchange-correlations gradient corrections); see also Table I.

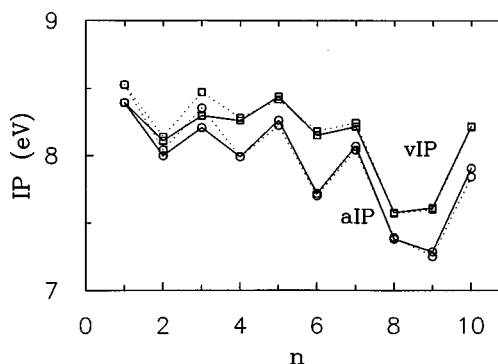FIG. 3. Vertical (vIP, squares) and adiabatic (aIP, circles) ionization potentials for Si_1–Si_{10}, in units of eV. Results are given from LSD (solid) and PLSD (dotted) calculations.

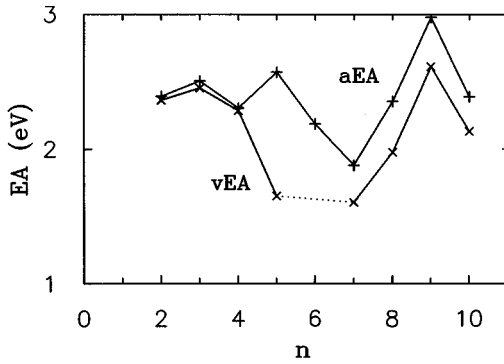FIG. 4. Vertical (vEA) and adiabatical (aEA) electron affinities of Si_2–Si_{10} in units of eV (the value of vEA for Si_6 has not been calculated due to technical difficulties). The results are given from LSD.

calculations for the hydrated Si_7NaH_2O cluster. The pseudopotential[34] core radii r_c are $r_c^{s,p,d}(Si)=2.10a_0$, $r_c^s(Na)=2.50a_0$, $r_c^p(Na)=2.75a_0$, $r_c^s(H)=0.95a_0$, and $r_c^{s,p}(O)=1.45a_0$, where s,p,d denote the angular momentum components.

III. RESULTS

A. Si_n ($n \leq 10$) clusters

The optimal geometries for Si_n ($n \leq 10$) clusters are shown in Fig. 1 and Table IV, and their energetics is given in Figs. 2–4 and in Table I. All the neutral clusters considered here have singlet ground electronic states except Si_2 ($^3\Sigma_g^-$ ground state). The optimal geometries for the neutral clusters correspond to the following: Si_3, a C_{2v} isosceles triangle; Si_4, a planar D_{2h} rhombus; Si_5, a flattened D_{3h} trigonal bipyramid [with the triangle atoms not bonded to each other, and the

apex atoms (4 and 5 in Fig. 1) separated by 2.91 Å]; Si_6, a C_{2v} edge-capped trigonal bipyramid, a close lying C_{2v} face-capped trigonal bipyramid isomer, and a higher-energy tetragonal bipyramidal one; Si_7, a D_{5h} pentagonal bipyramid; Si_8, a C_{2h} bicapped distorted octahedron; Si_9, a D_{3h} distorted tricapped prism and a close lying C_s distorted tricapped octahedral isomer; Si_{10}, a C_{3v} tetracapped trigonal prism and a close lying T_d tetracapped octahedral isomer. Interatomic distances and angles for the neutral clusters and for their cations and anions are given in Table IV. These geometries are in general agreement with those determined in earlier studies (see, e.g., Refs. 1, 2, 5, 8, and 18).

The energetics displayed in Figs. 2–4 and in Table I (where results are given from LSD calculations, as well as including PLSD xcg corrections, marked xcg) reveal the following trends.

(i) The total energy per atom ($E^{(n)}/n$ where $E^{(n)}$ is the total energy of a Si_n cluster, see Table I) and the atomization energy [$E_a^{(n)}=(E^{(n)}-nE^{(1)})/n$, see Fig. 2] ''saturate'' at $n \geq 6$. We note that even for $n=10$ the calculated atomization energy is much smaller than the calculated cohesive energy for bulk silicon (see Table III in Ref. 34, where a LDA value, without xcg corrections, of 8.80 eV is given) and the measured one (7.37 eV, see Ref. 37).

(ii) The ''adsorption'' energy (or monomer separation energy, i.e., the energy involved in the process, $Si_{n+1} \rightarrow Si_n + Si$, given by $\triangle^{(n)}=E^{(n+1)}-E^{(n)}-E^{(1)}$, see Fig. 2), shows local maxima for $n=4$, 7, and 10.

(iii) The vertical (vIP) and adiabatic (aIP) ionization potentials are smaller than those of the Si atom, and exhibit odd-even oscillations, (see Fig. 3). Our calculated aIP values are in very good agreement with those measured through near threshold photoionization,[30] superior to that achieved in a previous calculation.[32]

TABLE I. Energetics of Si_n ($1 \leq n \leq 10$) clusters (in units of eV). Total energy per atom, $E^{(n)}/n$; atomization energy, $E_a^{(n)}$; monomer separation (adsorption) energy, $\Delta^{(n)}$; vertical (vIP) and adiabatic (aIP) ionization potentials; cluster relaxation energy, $E_R=$vIP$-$aIP; vertical (vEA) and adiabatic (aEA) electronic affinities; negative ion cluster relaxation energy, $E_R^-=$aEA$-$vEA. Results are given for LSD and PLSD, i.e., including xcg correction in a PLSD mode.

| Si_n	1	2	3	4	5	6	7	8	9	10
$E^{(n)}/n$	−102.960	−105.038	−106.044	−106.675	−106.967	−107.194	−107.358	−107.299	−107.295	−107.546
$E^{(n)}/n$ (xcg)	−104.017	−105.936	−106.854	−107.394	−107.619	−107.811	−107.940	−107.879	−105.817	−108.081
$E_a^{(n)}$		2.078	3.085	3.716	4.007	4.234	4.398	4.339	4.335	4.586
$E_a^{(n)}$ (xcg)		1.918	2.837	3.376	3.602	3.794	3.923	3.861	3.845	4.063
$\Delta^{(n)}$		4.156	5.098	5.609	5.171	5.372	5.363	3.923	4.297	6.845
$\Delta^{(n)}$ (xcg)		3.836	4.674	4.995	4.503	4.754	4.696	3.433	3.718	6.025
vIP	8.395	8.109	8.297	8.261	8.440	8.151	8.214	7.577	7.612	8.219
vIP (xcg)	8.528	8.140	8.472	8.281	8.419	8.181	8.244	7.571	7.601	8.213
aIP	8.395	7.999	8.207	7.992	8.263	7.719	7.931	7.382	7.286	7.907
aIP (xcg)	8.528	8.042	8.355	7.991	8.224	7.702	8.041	7.393	7.252	7.843
E_R		0.111	0.090	0.270	0.177	0.432	0.145	0.196	0.326	0.312
E_R (xcg)		0.098	0.117	0.290	0.195	0.479	0.203	0.178	0.349	0.370
vEA		2.366	2.457	2.289	1.651		1.604	1.977	2.616	2.132
aEA		2.394	2.509	2.309	2.575	2.188	1.881	2.357	2.980	2.392
E_R^-		0.029	0.053	0.020	0.924		0.277	0.381	0.364	0.259
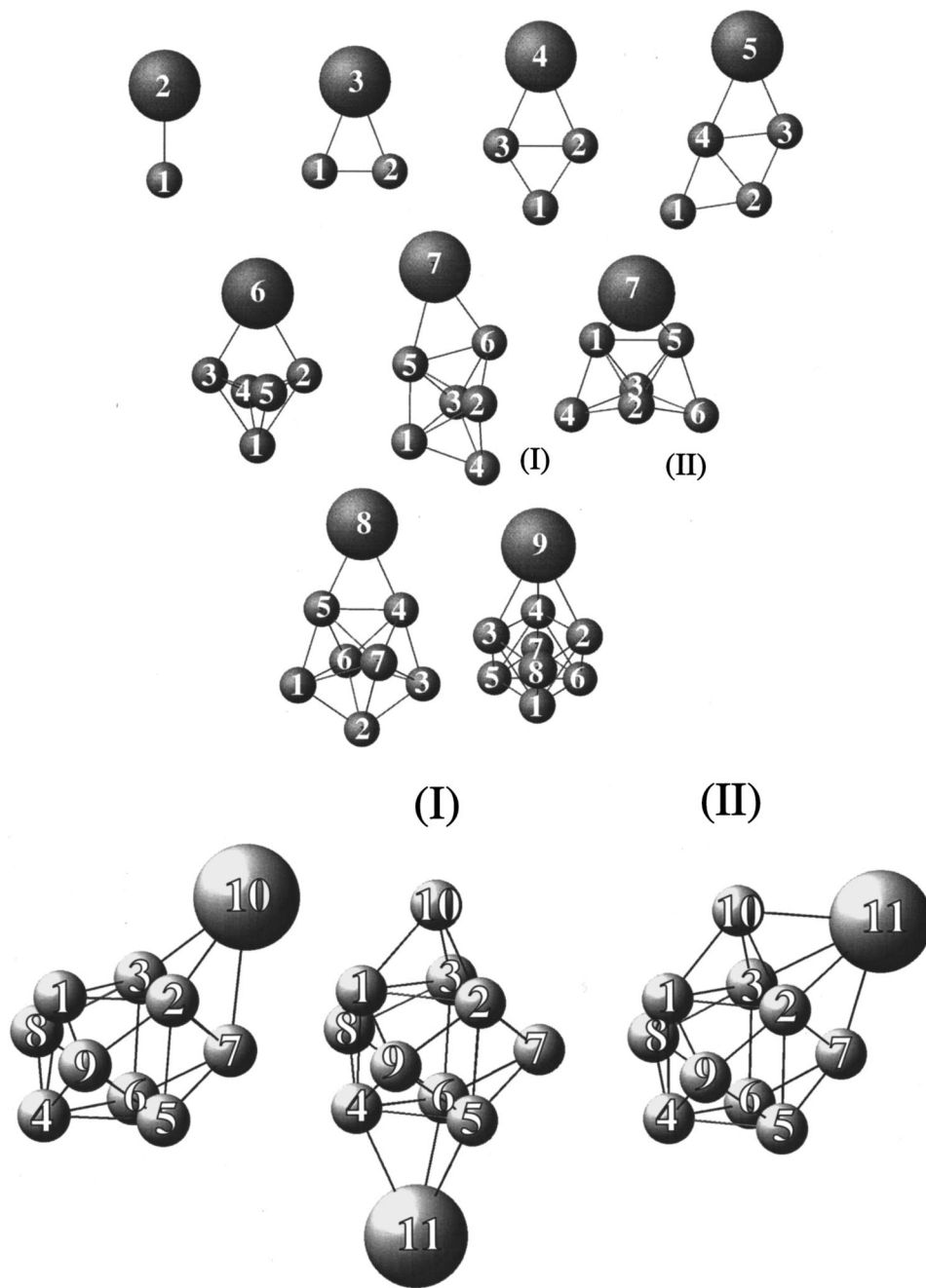
FIG. 5. Optimal geometries for neutral SiNa–Si$_{10}$Na doped clusters. The larger sphere represents the Na (the radii of the small and large sphere, are in the ratio of the radius of Si^{4+} and Na$^+$). For Si$_6$Na two isomers are shown, with the energy of Si$_6$Na(II) higher than that of Si$_6$Na(I) by 55 meV. Two isomers are also shown for Si$_{10}$Na, with the energy of Si$_{10}$Na(II) higher than that of Si$_{10}$Na(I) by 57 meV. For values of the interatomic distances see Table V, where the numbering of the atoms is as shown in the figure.
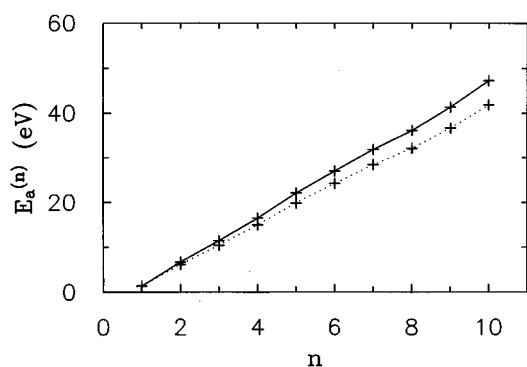
FIG. 6. Atomization energies, $E^{(n)} = E(Si_nNa) - nE(Si) - E(Na)$, for Si$_1$Na–Si$_{10}$Na clusters. Energies in units of eV are given from LSD (solid) and PLSD (dotted) calculations. See also Table II.
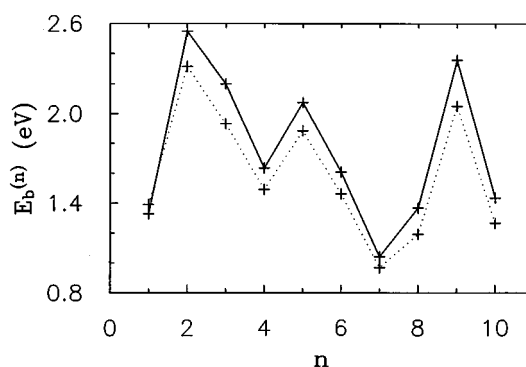
FIG. 7. Sodium binding energies, $E_b^{(n)} = E(Si_nNa) - E(Si_n) - E(Na)$, for Si$_1$Na–Si$_{10}$Na clusters. Energies in unit of eV are given from LSD (solid) and PLSD (dotted) calculations.

TABLE II. Energetics of sodium-doped Si_nNa ($1 \leq n \leq 10$) clusters (in units of eV). Total energy per atom, $E^{(n)}/n$; sodium binding energy (sodium adsorption energy), $E_b^{(n)}$; vertical (vIP) and adiabatic (aIP) ionization potentials; cluster relaxation energy, E_R; cluster dipole moment, μ (in a.u.); angle θ, between the dipole moment and the vector, R_d, connecting the center of mass of the silicon atoms in the cluster and the sodium atom; effective charge, $q = \mu/R_d$, in electron charge units. Results are given for LSD and PLSD, i.e., including xcg correction in a PLSD mode.

Si_nNa	1	2	3	4	5	6	7	8	9	10
$E^{(n)}/n$	−109.497	−108.918	−108.514	−108.386	−108.424	−108.330	−108.251	−108.121	−108.137	−108.210
$E^{(n)}/n$ (xcg)	−110.821	−109.800	−109.302	−109.120	−109.078	−108.957	−108.851	−108.704	−108.692	−108.749
$E_b^{(n)}$	1.328	2.550	2.200	1.635	2.076	1.608	1.041	1.369	2.359	1.435
$E_b^{(n)}$ (xcg)	1.392	2.317	1.933	1.492	1.885	1.461	0.968	1.193	2.052	1.266
vIP	6.325	7.235	7.032	6.174	7.277	6.155	5.787	6.281	7.010	6.159
vIP (xcg)	6.355	7.070	6.966	6.217	7.376	6.215	5.860	6.277	6.976	6.197
aIP	6.235	7.084	6.870	6.058	6.562	5.999	5.357	5.938	6.164	5.728
aIP (xcg)	6.281	6.940	6.792	6.114	6.609	6.055	5.459	5.971	6.208	5.772
E_R	0.090	0.150	0.163	0.115	0.715	0.156	0.431	0.344	0.846	0.431
E_R (xcg)	0.074	0.130	0.174	0.103	0.767	0.160	0.401	0.306	0.768	0.425
μ (a.u.)	2.253	2.693	3.170	3.733	2.875	3.861	3.854	3.291	3.445	2.979
θ (rad)	0.018	0.000	0.000	0.000	0.000	0.033	0.000	0.028	0.052	0.000
q	0.430	0.541	0.520	0.538	0.504	0.504	0.500	0.483	0.456	0.377

(iv) The vertical (vEA) and adiabatic (aEA) electron affinities of Si_n, $2 \leq n \leq 4$, are close to each other, corresponding to very small reorganization energies (E_R^- in Table I). The reorganization energies for clusters with $n \geq 5$ are larger. The aEA's for clusters with $n=4$, 7, and 10 are local minima, with those for Si_7 being the smallest in this range (see Fig. 4). The pattern exhibited by the calculated aEA's corresponds to that measured by photoelectron spectroscopy using an ArF excimer laser (6.42 eV),[26] and is also similar to that calculated in Ref. 8 (see also discussion there pertaining to the orbital origins of the observed trend); for Si_2 our calculated value for the vEA equals 2.4 eV, in good agreement with the measured[38] value (2.2 eV).

(v) The optimal geometries of the cationic (Si_n^+) and anionic (Si_n^-) clusters are similar to those of the corresponding neutral ones, see Table IV, the largest reorganization occurs upon formation of the Si_5^- anion (see also Ref. 8 where a similar result has been obtained).

B. Si_nNa ($n \leq 10$) clusters

The optimal geometries of the Si_nNa clusters are displayed in Fig. 5, and the geometrical parameters are given in Table V for both neutral and ionized sodium-doped clusters. The optimal geometries shown correspond to bond capped (Si_2Na); edge capped (Si_3Na); edge-capped distorted rhombus (Si_4Na); edge-capped trigonal bipyramid (Si_5Na); edge capping of the face-capped trigonal bipyramid and a face-capped isomer (Si_6Na); edge capped trigonal bipyramid (Si_7Na); edge capping of the bicapped distorted octahedron (Si_8Na); face capping of the tricapped distorted trigonal prism (Si_9Na); face capping of the tetracapped distorted trigonal prism (I), and a face- and edge-capping of the tetracapped distorted trigonal prism (II), ($Si_{10}Na$).

The energetics of the Si_nNa clusters given in Table II and shown in Figs. 6–8, exhibits the following trends.

(i) The atomization energy, $E_a^{(n)} = E(Si_nNa) - nE(Si) - E(Na)$, where $E(Si_nNa)$ is the total energy of the Si_nNa clusters, increases monotonically with n (see Fig. 6).

(ii) The binding of Na to Si_n clusters, $E_b^{(n)} = E(Si_nNa) - E(Si_n) - E(Na)$, oscillates as a function of n, showing local maxima for $n=2$, 5, and 9, and local minima for $n=4$, 7, and 10 (see Fig. 7).

(iii) The ionization potentials for the sodium-doped clusters are significantly lower than those for the parent Si_n clusters. The decrease reflects the change in the orbital being ionized, which in the sodium-doped cluster is of similar character as the lowest unoccupied orbital of the parent Si_n cluster.[32] Our results are in agreement with experimentally measured IP's.[31,32] The above trends in the sodium binding energies to the silicon clusters are also found for the vIP's and aIP's of the Si_nNa clusters (Fig. 8), which are the small-
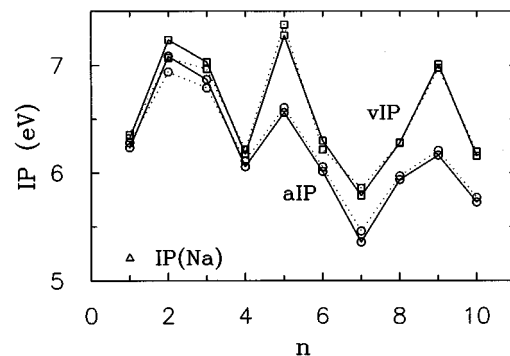

FIG. 8. Vertical (vIP, squares) and adiabatic (aIP, circles) ionization potential energies for Si_1Na–$Si_{10}Na$ clusters. Energies in units of eV are given from LSD (solid) and PLSD (dotted) calculations. The calculated ionization potential of a sodium atom IP(Na) =5.21 eV is given by the triangle, and the calculated ionization potential of a silicon atom is 8.38 eV.
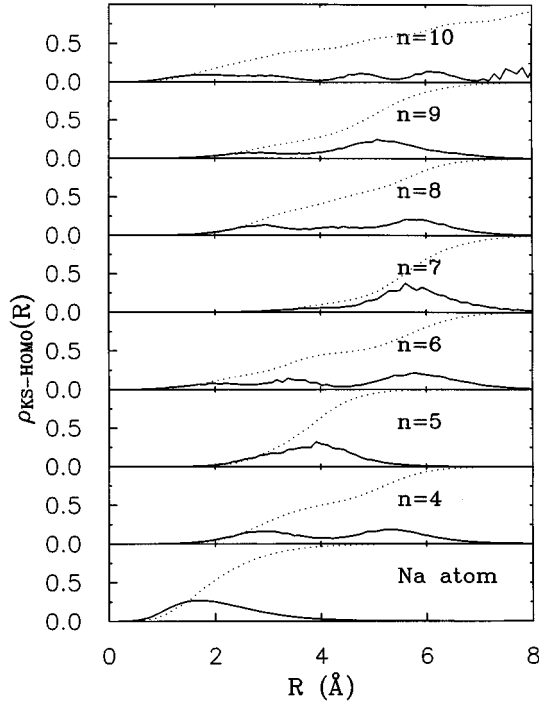
FIG. 9. Radial $\rho(R)$ (solid) and integrated $\bar{\rho}(R)$ (dotted) electronic charge density plots for the KS-HOMO orbital in Si_nNa clusters, evaluated about the Na nucleus in the doped cluster. Corresponding plots for the sodium atom are shown at the bottom. Distance, R, in units of Å.
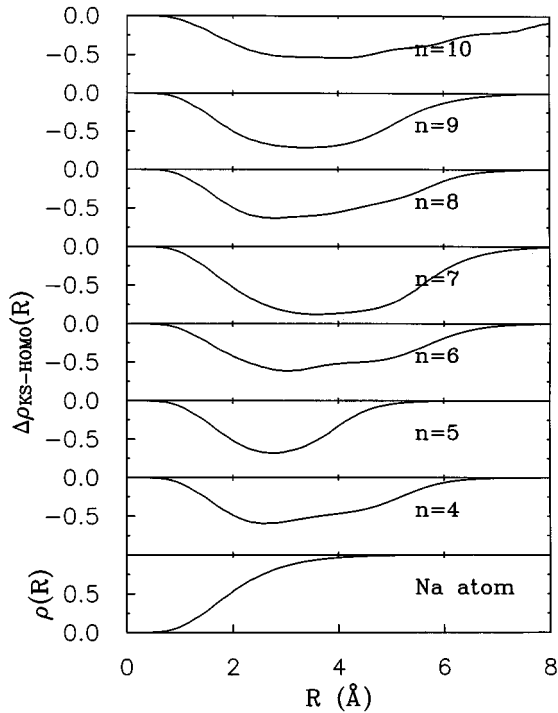

FIG. 10. Electron density difference plots, $\Delta\rho(R) = \int_0^R [\rho_{Si_nNa}(r) - \rho_{Na}(r)] dr$, for the KS-HOMO orbital of the doped cluster (and the free Na atom), evaluated about the Na as the origin. The integrated electron density of an isolated Na atom is shown at the bottom. Distance R in units of Å.

TABLE III. Energetics of Si_7NaH_2O (lowest-energy isomer, I in Fig. 11) and NaH_2O (in units of eV). Binding energies of H_2O to Na and to Si_7Na, E_b, and to the ionized species, E_b^+; vertical (vIP) and adiabatic (aIP) ionization potentials. Results are given for LSD and PLSD, i.e., including xcg correction a PLSD mode. The values for the NaH_2O system are from Ref. 39. These values are in very good agreement with measured (Ref. 40) ones for this system, i.e., $E_b=0.28\pm0.04$ eV, $E_b^+=1.04$ eV, aIP=4.38$\pm$0.03 eV.

	NaH_2O	Si_7NaH_2O
Binding energies of H_2O		
E_b	0.40	0.68
E_b (xcg)	0.27	0.57
Ionization energies		
vIP	4.62	5.61
vIP (xcg)	4.62	5.67
aIP	4.55	5.14
aIP (xcg)	4.62	5.24
Binding energies of H_2O to the ionized cluster		
E_b^+	1.06	0.78
E_b^+ (xcg)	1.06	0.70

est for $n=7$, as observed experimentally. Si_n clusters characterized as local minima in the size evolution of the electron affinities (Fig. 4), correspond to local minima in the sodium binding energies (Fig. 7) and to local aEA (and vEA) minima of the corresponding doped Si_nNa clusters [with the smallest aIP obtained for Si_7Na (see Fig. 8)]. These results are in agreement with experiments (see Fig. 2 in Ref. 32), superior to that obtained by previous restricted Hartree-Fock calculations[32] for Si_nNa ($n=1-7$).
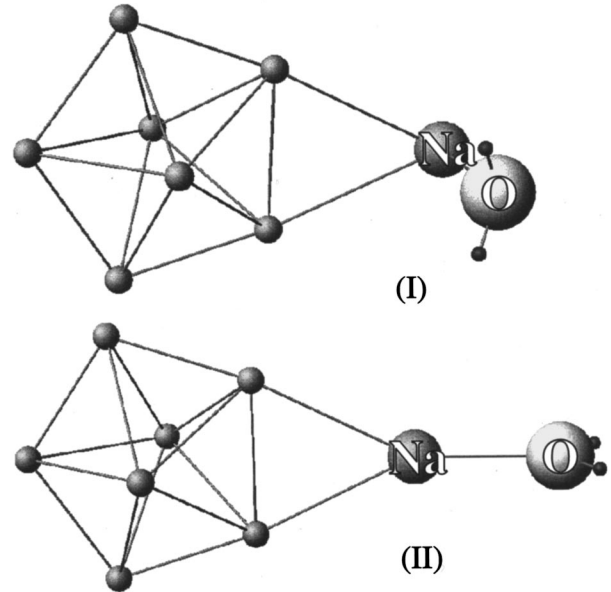
FIG. 11. Two low energy geometries of the hydrated silicon heptamer, $Si_7Na(H_2O)(I)$ and $Si_7Na(H_2O)(II)$. For $Si_7Na(H_2O)(I)$ $d_{Na-O}=2.31$ Å, the angle between the Na-O bond and the normal to the plane defining the base of the silicon pentagonal bipyramid is $\alpha=0.09$ rad (5.16°), and the angle between the bisector or the HOH angle and the vector connecting the sodium and oxygen atoms is $\beta=3.08$ rad (176.6°). For $Si_7Na(H_2O)(II)$ $d_{Na-O}=2.24$ Å, and $\alpha=90°$, $\beta=180°$.

TABLE IV. Interatomic distances for optimized geometries of Si_n, Si_n^+, Si_n^-, in units of a_0 (bohr radius). The identities of the atoms are as shown in Fig. 1.

n		Si_n	Si_n^+	Si_n^-	n		Si_n	Si_n^+	Si_n^-
2		$r_{12}=3.99$	4.24	3.98			$r_{46}=4.53$	4.51	4.62
3	C_{2v}	$r_{12}=4.09$	4.33	4.31			$r_{47}=r_{56}=r_{57}=r_{46}$		
		$r_{13}=r_{12}$					$r_{67}=4.60$	4.71	5.21
		$r_{23}=4.60$	4.00	4.12	8	C_{2h}	$r_{12}=4.52$	4.56	4.78
4	D_{2h}	$r_{12}=4.28$	4.23	4.27			$r_{13}=r_{45}=r_{46}=r_{12}$		
		$r_{34}=r_{23}=r_{14}=r_{12}$					$r_{15}=4.45$	4.43	4.49
		$r_{24}=4.42$	4.87	4.31			$r_{16}=r_{24}=r_{34}=r_{15}$		
5	D_{3h}	$r_{14}=4.25$	4.44	4.30			$r_{81}=4.19$	4.32	4.27
		$r_{15}=r_{14}$					$r_{74}=r_{81}$		
		$r_{24}=4.25$	4.23	4.30			$r_{82}=4.51$	4.50	4.40
		$r_{25}=r_{34}=r_{35}=r_{24}$					$r_{83}=r_{75}=r_{74}=r_{82}$		
		$r_{45}=5.50$	5.86	6.38	9	C_{2h}	$r_{12}=4.70$	4.88	4.84
6(I)	C_{2v}	$r_{12}=4.35$	4.71				$r_{13}=r_{45}=r_{46}=r_{12}$		
		$r_{13}=r_{12}$					$r_{23}=4.66$	4.85	4.58
		$r_{14}=4.45$	4.48				$r_{56}=r_{23}$		
		$r_{15}=r_{14}$					$r_{14}=4.51$	4.46	4.61
		$r_{25}=4.43$	4.32				$r_{25}=4.54$	4.47	4.61
		$r_{35}=r_{24}=r_{34}=r_{25}$					$r_{36}=r_{25}$		
		$r_{26}=4.27$	4.37				$r_{18}=4.56$	4.56	4.48
		$r_{36}=r_{26}$					$r_{19}=r_{48}=r_{49}=r_{18}$		
6(II)	C_{2v}	$r_{12}=4.83$					$r_{29}=4.55$	4.55	4.57
		$r_{13}=r_{12}$					$r_{38}=r_{59}=r_{68}=r_{29}$		
		$r_{23}=4.73$					$r_{27}=4.55$	4.56	4.49
		$r_{14}=4.43$					$r_{37}=r_{57}=r_{67}=r_{27}$		
		$r_{24}=4.49$			10	C_{2h}	$r_{12}=4.96$	4.97	4.74
		$r_{34}=r_{22}$					$r_{13}=r_{12}$		
		$r_{15}=4.15$					$r_{45}=4.66$	4.49	4.60
		$r_{25}=4.44$					$r_{46}=r_{45}$		
		$r_{35}=r_{25}$					$r_{23}=4.94$	4.97	4.73
		$r_{56}=4.43$					$r_{56}=4.65$	4.49	4.61
		$r_{26}=4.49$					$r_{14}=4.57$	4.60	4.76
		$r_{36}=r_{26}$					$r_{25}=4.57$	4.58	4.77
6(III)		$r_{12}=5.11$					$r_{36}=r_{25}$		
		$r_{23}=r_{34}=r_{14}=r_{12}$					$r_{18}=4.49$	4.50	4.46
		$r_{15}=4.36$					$r_{19}=r_{18}$		
		$r_{25}=r_{35}=r_{45}=r_{15}$					$r_{48}=4.55$	4.57	4.53
		$r_{16}=r_{26}=r_{36}=r_{46}=r_{15}$					$r_{49}=r_{48}$		
		$r_{56}=4.88$					$r_{29}=4.49$	4.57	4.46
7	D_{5h}	$r_{12}=4.59$	4.83	4.49			$r_{38}=r_{29}$		
		$r_{23}=r_{12}$					$r_{59}=4.53$	4.50	4.54
		$r_{34}=4.59$	4.43	4.49			$r_{68}=r_{59}$		
		$r_{15}=r_{34}$					$r_{27}=4.50$	4.51	4.46
		$r_{45}=4.59$	4.34	4.49			$r_{37}=r_{27}$		
		$r_{16}=4.53$	4.49	4.62			$r_{57}=4.54$	4.59	4.54
		$r_{17}=r_{36}=r_{37}=r_{16}$					$r_{67}=r_{57}$		
		$r_{26}=4.53$	4.61	4.62			$r_{1,10}=4.30$	4.32	4.39
		$r_{27}=r_{26}$					$r_{2,10}=r_{3,10}$		

TABLE V. Interatomic distances for optimized geometries of Si_nNa, Si_nNa^+ in units of a_0 (bohr radius). The identities of the atoms are as shown in Fig. 5.

n	Si_nNa	Si_nNa^+
1	$r_{12}=5.24$	5.85
2	$r_{12}=3.91$	4.03
	$r_{13}=5.35$	5.96
	$r_{23}=r_{13}$	
3	$r_{12}=4.10$	4.25
	$r_{13}=r_{12}$	
	$r_{23}=4.42$	4.15
	$r_{24}=5.42$	5.47
	$r_{34}=r_{24}$	
4	$r_{24}=4.28$	4.36
	$r_{12}=4.25$	4.34
	$r_{23}=4.19$	4.21
	$r_{34}=4.41$	4.31
	$r_{41}=4.29$	4.29
	$r_{35}=5.15$	5.74
	$r_{45}=5.68$	5.92
5	$r_{14}=4.40$	4.20
	$r_{15}=r_{14}$	
	$r_{24}=4.30$	4.24
	$r_{34}=r_{25}=r_{35}=r_{24}$	
	$r_{45}=6.50$	5.64
	$r_{26}=5.27$	5.53
	$r_{36}=r_{26}$	
6(I)	$r_{12}=4.41$	4.39
	$r_{13}=r_{12}$	
	$r_{23}=4.65$	4.84
	$r_{24}=4.57$	4.48
	$r_{34}=r_{24}$	
	$r_{25}=4.31$	4.32
	$r_{35}=r_{35}$	
	$r_{14}=4.48$	4.73
	$r_{26}=4.55$	4.42
	$r_{36}=r_{26}$	
	$r_{56}=4.73$	4.74
	$r_{57}=5.23$	5.70
	$r_{67}=5.57$	5.99
6(II)	$r_{12}=4.58$	4.49
	$r_{52}=r_{12}$	
	$r_{13}=4.65$	4.38
	$r_{53}=r_{13}$	
	$r_{23}=4.56$	4.80
	$r_{14}=4.50$	4.80
	$r_{56}=r_{14}$	
	$r_{24}=4.44$	4.38
	$r_{26}=r_{24}$	
	$r_{34}=4.41$	4.39
	$r_{36}=r_{34}$	
	$r_{17}=5.36$	5.87
	$r_{57}=r_{17}$	
	$r_{27}=6.45$	6.38
7	$r_{12}=4.59$	4.59
	$r_{23}=r_{12}$	
	$r_{34}=4.59$	4.48
	$r_{15}=r_{34}$	
	$r_{45}=4.71$	4.74
	$r_{16}=4.53$	4.59
	$r_{17}=r_{36}=r_{37}=r_{16}$	
	$r_{26}=4.53$	4.53
	$r_{27}=r_{26}$	
	$r_{46}=4.53$	4.48
	$r_{56}=r_{47}=r_{57}=r_{46}$	
	$r_{67}=4.60$	4.65
	$r_{48}=5.28$	5.69
	$r_{58}=r_{46}$	

n	Si_nNa	Si_nNa^+
8	$r_{12}=4.57$	4.54
	$r_{13}=4.57$	4.46
	$r_{18}=4.23$	4.20
	$r_{28}=4.43$	4.52
	$r_{38}=4.43$	4.54
	$r_{45}=4.62$	4.55
	$r_{46}=4.62$	4.40
	$r_{47}=4.23$	4.22
	$r_{57}=4.41$	4.62
	$r_{67}=4.41$	4.56
	$r_{78}=10.54$	10.72
	$r_{29}=5.51$	5.34
	$r_{39}=5.51$	9.63
	$r_{49}=5.68$	5.41
9	$r_{12}=4.71$	4.66
	$r_{13}=4.64$	4.57
	$r_{45}=4.95$	
	$r_{46}=4.52$	4.48
	$r_{23}=4.89$	
	$r_{56}=4.87$	4.74
	$r_{14}=4.61$	4.51
	$r_{25}=4.58$	4.62
	$r_{36}=4.57$	4.80
	$r_{18}=4.39$	4.34
	$r_{19}=4.53$	4.75
	$r_{48}=4.61$	4.73
	$r_{49}=4.69$	4.74
	$r_{29}=4.59$	4.55
	$r_{38}=4.54$	4.64
	$r_{59}=4.41$	4.45
	$r_{68}=4.45$	4.35
	$r_{27}=4.60$	4.49
	$r_{37}=4.70$	4.80
	$r_{57}=4.37$	4.35
	$r_{67}=4.50$	4.47
	$r_{2,10}=5.41$	5.87
	$r_{3,10}=5.63$	
	$r_{7,10}=5.49$	5.70
10(I)	$r_{12}=4.78$	4.99
	$r_{13}=r_{13}$	
	$r_{45}=4.64$	4.70
	$r_{46}=r_{45}$	
	$r_{23}=4.76$	4.98
	$r_{56}=4.63$	4.68
	$r_{14}=4.65$	4.50
	$r_{25}=4.66$	4.51
	$r_{36}=4.66$	4.51
	$r_{18}=4.47$	4.51
	$r_{19}=r_{18}$	
	$r_{48}=4.53$	4.57
	$r_{49}=r_{48}$	
	$r_{29}=4.47$	4.50
	$r_{38}=r_{29}$	
	$r_{59}=4.53$	4.54
	$r_{68}=r_{59}$	
	$r_{27}=4.47$	4.51
	$r_{37}=r_{37}$	
	$r_{67}=4.54$	4.55
	$r_{57}=r_{57}$	
	$r_{1,10}=4.37$	4.29
	$r_{2,10}=4.37$	4.29
	$r_{3,10}=r_{2,10}$	
	$r_{4,11}=5.64$	5.81
	$r_{5,11}=5.68$	5.85
	$r_{6,11}=r_{5,11}$	

Further insights into the nature of bonding of Na to the silicon clusters are provided through inspection of the Kohn-Sham energy level schemes for Si_n, Si_n^-, and Si_nNa (not shown), plots of the spherically averaged radial electron density, $\rho(R)$, of the highest-occupied molecular orbital (KS-HOMO), and of the integrated KS-HOMO radial density, $\bar{\rho}(R)$, shown in Fig. 9, and plots of the integrated radial density difference, $\Delta\rho(R)$, displayed in Fig. 10. From the KS level schemes we observed that while in the ground state a Si atom has two unpaired electrons, only one electron is unpaired in the SiNa molecule, and similarly for Si_2 and Si_2Na. We also noted that the adsorption of Na is accompanied by small changes in the positions of the levels of the corresponding bare clusters.

For the Si_nNa cluster with $n \geqslant 4$ the KS orbital which is occupied by the added electron (i.e., the Na electron) can be readily distinguished as the KS-HOMO whose character is similar to that of the KS lowest unoccupied molecular orbital (KS-LUMO) of the corresponding Si_n cluster. The plots in Fig. 9 of $\rho(R)$ and $\bar{\rho}(R) = \int_0^R \rho(r)dr$, both calculated for the KS-HOMO with the Na atom as the origin, illustrate that the electron density in the vicinity of the sodium is depleted. This is also evident in Fig. 10 from the electron density difference plots, $\Delta\rho(R) = \int_0^R [\rho_{Si_nNa}(r) - \rho_{Na}(r)]dr$, for the KS-HOMO orbital of the clusters, evaluated about the Na atom as the origin. From these plots it is observed that the electron density depletion about the Na is largest for Si_7Na.

The donation of the electron from the Na to the silicon cluster leads to the development of a dipole moment μ, showing an overall increasing trend with n (see Table II). For all the clusters the dipole is essentially parallel to the vector R_d connecting the center of mass of the silicon atoms and the sodium nucleus in the doped cluster (see θ in Table II). Associated with the dipole moments are effective charges calculated as $q = \mu/R_d$, which for $1 \leqslant n \leqslant 10$ range between $0.38e$ and $0.54e$, with a decreasing trend for the larger clusters.

IV. SUMMARY AND WATER MOLECULE ADSORPTION ON Si_7Na

In this study the optimal geometries and energetics of Si_n, Si_n^+, Si_n^-, $2 \leqslant n \leqslant 10$ clusters, and of sodium-doped Si_nNa, $1 \leqslant n \leqslant 10$, clusters, have been studied using LSD and PLSD (i.e., including xcg in a LSD mode) calculations, employing the BO-LSD-MD method.[33]

As described in Sec. III the results and trends obtained for the Si_n clusters are in good agreement with available experimental data (ionization potentials[30] and electron affinities[26]), as well as in general agreement with previous calculations (particularly those using high-level quantum-chemistry methods, Refs. 1, 2, 5, and 8). The results for the sodium-doped, Si_nNa clusters show that the binding energy of Na to Si_n oscillates as a function of n, exhibiting local maxima for $n = 2, 5,$ and 9, and local minima for $n = 4, 7,$ and 10, with the value for $n = 7$ being the smallest (see Fig. 7). These trends are found also for the vertical and adiabatic ionization potentials (see vIP and aIP in Fig. 8), correlating with similar trends in the electron affinities of the parent Si_n clusters (see Fig. 4). This correlation reflects the nature of binding of Na to Si_n, which is found to involve transfer of charge from the

sodium to the Si_n (i.e., formation of a highly ionic bond), with the KS-HOMO in Si_nNa of similar character as the KS-LUMO in the parent Si_n. This leads to the development of relatively large dipole moments for the Si_nNa clusters. Our results are in good agreement with measured ionization potentials (Ref. 31, and in Fig. 2 in Ref. 32) for Si_nNa, superior to that obtained by previous calculations.[32]

In light of the unique characteristics of Si_7Na (having the smallest vIP and aIP values in the sequence of clusters studied, as well as the smallest Na binding energy), we investigated for it the geometry and energetics of hydration, i.e., formation of Si_7NaH_2O. Motivating this study is the aforementioned observations that the binding of Na to the silicon cluster involves transfer of the sodium electron into the silicon cluster, resulting in a high partial positive charge on the attached sodium. Since the hydration energy of sodium is very sensitive to its charge state[39,40] (i.e., the binding energy of H_2O to Na is more than doubled when H_2O is bonded to Na^+, see Table III), it is of interest to explore hydration of Na-doped silicon clusters and the effect of charging (i.e., ionization of the doped cluster) on the hydration energies.

The ground-state optimal structure of Si_7NaH_2O and a close lying isomer are shown in Fig. 11, the total energy of the isomer (II) is 50 meV higher than that of the ground-state one (I). Other adsorption geometries, where the water molecule is bonded directly to the Si_7 fragment of the Si_7Na cluster, result in much higher total energies. From the results given in Table III we conclude the following.

(i) The hydration energy of Si_7NaH_2O is significantly higher than that of an isolated sodium atom.

(ii) Ionization of hydrated Si_7NaH_2O results in an increase of ≈ 0.13 eV in the binding energy of H_2O to the ionized cluster (i.e., the hydration energy of Si_7Na^+ is increased by that amount compared to the hydration of the neutral). On the other hand, the hydration energy of Na^+ is a factor of 4 larger than that of the neutral Na atom. These results correlate with the observation that in Si_7Na the sodium is bonded in a highly ionic (positively charged) state, via transfer of the electron to the silicon cluster, resulting in a relatively small effect of the ionization of the cluster on the hydration energy (compared to the case of the individual sodium).

(iii) The ionization potentials (vIP and aIP) of NaH_2O are lower than those of the hydrated Si_7NaH_2O cluster, and the values for the latter are lower by ≈ 0.2 eV than those corresponding to the unhydrated Si_7Na cluster. Consequently, water molecular attachment to the cluster may be detected via ionization potential measurements.

APPENDIX

In this appendix interatomic distances for Si_n, Si_n^+, and Si_n^- ($n \leqslant 10$) clusters are given in Table IV (see correspond-

ing configurations in Fig. 1); interatomic distances for Si_nNa and Si_nNa^+ clusters are given in Table V (see corresponding configurations in Fig. 5).

As aforementioned, the optimized geometries which we list are from LSD calculations. Geometries optimized using LSD including xcg corrections are of the same symmetry with slightly increased interatomic distances; for example,

for the tetramer, the LSD-xcg r_{12} and r_{24} bond lengths in both Si_4 and Si_4^+ are larger by 2–3 % than those given in Table IV. Similarly, the ionization potentials from LSD-xcg calculations are decreased by $\sim$2–3 % compared to those obtained by us using PLSD-xcg calculations (see Table I, and Fig. 3). These variations do not affect the trends and other findings of our study.

[1] K. Raghavachari and V. Logovinsky, Phys. Rev. Lett. **55**, 2853 (1985).

[2] K. Raghavachari, J. Chem. Phys. **84**, 5672 (1986).

[3] For earlier work see Refs. 12–23 cited in Ref. 2.

[4] D. Tomanek and M. Schluter, Phys. Rev. Lett. **56**, 1055 (1986); Phys. Rev. B **36**, 1208 (1987); Phys. Rev. Lett. **67**, 2331 (1991).

[5] K. Raghavachari and C. M. Rohlfing, J. Chem. Phys. **89**, 2219 (1988).

[6] P. Ballone, W. Andreoni, R. Car, and M. Parrinello, Phys. Rev. Lett. **60**, 271 (1988); W. Andreoni and G. Pastore, Phys. Rev. B **41**, 10 243 (1990).

[7] J. R. Chelikowsky and J. C. Philips, Phys. Rev. Lett. **63**, 1653 (1989).

[8] K. Raghavachari and C. M. Rohlfing, J. Chem. Phys. **94**, 3670 (1991); for earlier work on neutral clusters see also Refs. 16–30 cited in this paper.

[9] U. Rothlisberger, W. Andreoni, and P. Giannozzi, J. Chem. Phys. **92**, 1248 (1992).

[10] N. Binggeli, J. L. Martins, and J. R. Chelikowsky, Phys. Rev. Lett. **68**, 2956 (1992).

[11] E. Kaxiras and K. Jackson, Phys. Rev. Lett. **71**, 727 (1993).

[12] J. C. Philips, Phys. Rev. B **47**, 14 132 (1993).

[13] M. Menon and K. R. Subbaswamy, Phys. Rev. B **47**, 12 754 (1993); Chem. Phys. Lett. **219**, 219 (1994).

[14] P. Ordejon, D. Lebedenko, and M. Menon, Phys. Rev. B **50**, 5645 (1994).

[15] J. Pan and M. V. Ramakrishna, Phys. Rev. B **50**, 15 431 (1994).

[16] N. Binggeli and J. R. Chelikowsky, Phys. Rev. B **50**, 11 764 (1994).

[17] X. Jing, N. Troullier, D. Dean, N. Binggeli, R. Chelikowsky, K. Wu, and Y. Saad, Phys. Rev. B **50**, 12 234 (1994); N. Binggeli and J. R. Chelikowsky, Phys. Rev. Lett. **75**, 493 (1995).

[18] J. C. Grossman and L. Mitas, Phys. Rev. Lett. **74**, 1323 (1995).

[19] K. Kobayashi and S. Nagase, Bull. Chem. Soc. Jpn. **66**, 3334 (1993).

[20] R. E. Honig, J. Chem. Phys. **22**, 1610 (1954).

[21] T. T. Tsong, Appl. Phys. Lett. **45**, 1149 (1984); Phys. Rev. B **30**, 4946 (1984).

[22] L. A. Bloomfield, R. R. Freeman, and W. L. Brown, Phys. Rev. Lett. **54**, 2246 (1985); L. A. Bloomfield, M. E. Geusic, R. R. Freeman, and W. L. Brown, Chem. Phys. Lett. **121**, 33 (1985).

[23] J. R. Heath, Y. Liu, S. C. O'Brien, Q.-L. Zhang, R. F. Curl, F. K. Tittel, and R. E. Smalley, J. Chem. Phys. **83**, 5520 (1985).

[24] W. L. Brown, R. R. Freeman, K. Raghavachari, and M. Schluter, Science **235**, 860 (1987).

[25] M. F. Jarrold and J. E. Brown, J. Chem. Phys. **92**, 5702 (1988).

[26] O. Cheshnovsky, S. H. Yang, C. L. Pettiette, M. J. Craycraft, Y. Liu, and R. E. Smalley, Chem. Phys. Lett. **138**, 119 (1987).

[27] M. F. Jarrold, J. E. Brown, and K. M. Creegan, J. Chem. Phys. **90**, 3615 (1989); K. M. Creegan and M. F. Jarrold, J. Am. Chem. Soc. **112**, 3768 (1990); M. F. Jarrold, U. Ray, and K. M. Creegan, J. Chem. Phys. **93**, 224 (1990).

[28] M. F. Jarrold, Science **252**, 1085 (1991).

[29] E. C. Honea et al., Nature (London) **366**, 42 (1993).

[30] K. Fuke, K. Tsukamato, F. Misiazu, and M. Sanekata, J. Chem. Phys. **99**, 7807 (1993).

[31] K. Kaya, T. Sugioka, T. Taguwa, K. Hoshino, and A. Nakajima, Z. Phys. D **26**, 5201 (1993).

[32] R. Kishi, A. Nakajima, S. Iwata, and K. Kaya, Chem. Phys. Lett. **224**, 200 (1994); for an updated version of the experimental results for Si_nNa ($n = 2$–7) see Fig. 2 in this paper [compare with Fig. 1(a) in Ref. 31].

[33] R. N. Barnett and U. Landman, Phys. Rev. B **48**, 2081 (1993).

[34] N. Troullier and J. L. Martins, Phys. Rev. B **43**, 1993 (1991).

[35] A. D. Becke, Phys. Rev. A **38**, 3098 (1988); J. Chem. Phys. **96**, 2155 (1992).

[36] J. P. Perdew, Phys. Rev. B **33**, 8822 (1986); ibid. **34**, 7046 (1986).

[37] Numerical Data and Functional Relationships in Science and Technology, Landolt-Bornstein, edited by O. Madelung, New Series, Group III, Vol. 17, pt. a (Springer, Berlin, 1982).

[38] For measurement of the adiabatic electron affinity of Si_2, see M. R. Nimds, L. B. Harding, and G. B. Ellison, J. Chem. Phys. **87**, 5116 (1987).

[39] R. N. Barnett and U. Landman, Phys. Rev. Lett. **70**, 1775 (1993).

[40] C. P. Schulz, R. Haugstatter, H.-U. Tittes, and I. V. Hertel, Z. Phys. D **10**, 279 (1988); I. V. Hertel, C. Huglin, C. Nitsch, and C. P. Schulz, Phys. Rev. Lett. **67**, 1767 (1991).